



New Opportunities Offered by the ESRF to the Cultural and Natural Heritage Communities

Marine Cotte, Kathleen Dollman, Vincent Fernandez, Victor Gonzalez, Frederik Vanmeert, Letizia Monico, Catherine Dejoie, Manfred Burghammer, Loïc Huder, Stuart Fisher, Wout de Nolf, Ida Fazlic, Hiram Castillo-Michel, Murielle Salomé, Marta Ghirardello, Daniela Comelli, Olivier Mathon & Paul Tafforeau

To cite this article: Marine Cotte, Kathleen Dollman, Vincent Fernandez, Victor Gonzalez, Frederik Vanmeert, Letizia Monico, Catherine Dejoie, Manfred Burghammer, Loïc Huder, Stuart Fisher, Wout de Nolf, Ida Fazlic, Hiram Castillo-Michel, Murielle Salomé, Marta Ghirardello, Daniela Comelli, Olivier Mathon & Paul Tafforeau (2022) New Opportunities Offered by the ESRF to the Cultural and Natural Heritage Communities, *Synchrotron Radiation News*, 35:5, 3-9, DOI: [10.1080/08940886.2022.2135958](https://doi.org/10.1080/08940886.2022.2135958)

To link to this article: <https://doi.org/10.1080/08940886.2022.2135958>



© 2022 The Author(s). Published with license by Taylor & Francis Group, LLC.



Published online: 16 Nov 2022.



Submit your article to this journal [↗](#)



Article views: 264



View related articles [↗](#)



View Crossmark data [↗](#)

New Opportunities Offered by the ESRF to the Cultural and Natural Heritage Communities

MARINE COTTE,^{1,2} KATHLEEN DOLLMAN,¹ VINCENT FERNANDEZ,¹ VICTOR GONZALEZ,³ FREDERIK VANMEERT,^{4,5} LETIZIA MONICO,^{6,7,4} CATHERINE DEJOIE,¹ MANFRED BURGHAMMER,¹ LOÏC HUDER,¹ STUART FISHER,¹ WOUT DE NOLF,¹ IDA FAZLIC,^{1,8} HIRAM CASTILLO-MICHEL,¹ MURIELLE SALOMÉ,¹ MARTA GHIRARDELLO,⁹ DANIELA COMELLI,⁹ OLIVIER MATHON,¹ AND PAUL TAFFOREAU¹

¹European Synchrotron Radiation Facility (ESRF), Grenoble, France

²Sorbonne Université, CNRS, Laboratoire d'Archéologie Moléculaire et Structurale (LAMS), Paris, France

³Université Paris-Saclay, ENS Paris-Saclay, CNRS, PPSM, Gif-sur-Yvette, France

⁴Antwerp X-ray Imaging and Spectroscopy Laboratory (AXIS) Research Group, NANOLab Centre of Excellence, University of Antwerp, Antwerp, Belgium

⁵Paintings Laboratory, Royal Institute for Cultural Heritage (KIK-IRPA), Brussels, Belgium

⁶CNR-SCITEC, Perugia, Italy

⁷Centre of Excellence SMAArt, University of Perugia, Perugia, Italy

⁸Science Department, Rijksmuseum, Amsterdam, The Netherlands

⁹Physics Department, Politecnico di Milano, Milano, Italy

Introduction

For the past 20 years, the community of heritage scientists has frequently exploited the synchrotron radiation-based techniques offered at the European Synchrotron Radiation Facility (ESRF), Grenoble, France [1]. X-ray imaging techniques (in particular, micro computed-tomography, μ CT) are regularly employed to probe non-destructively the inner structure of objects and materials. In paleontology, this can offer information on the functioning and evolution of organs and organisms. In addition, analytical techniques such as X-ray fluorescence (XRF), X-ray powder diffraction (XRPD), and X-ray absorption spectroscopy (XAS) are often used, alone or combined, for the chemical analysis of micro-fragments of historical manufactured materials. This can give clues about both the early days of objects (physical and chemical processes used in the production of artworks and the evolution of these skills in time and space) as well as the evolution/alteration of objects (nature of degradation products and environmental factors contributing to these degradations). The limited size of samples and their high heterogeneity often require access to micro and nano-probes.

The new capabilities offered by the ESRF upgrade “EBS” (Extremely Brilliant Source), as well as instrumental developments at new and strongly refurbished beamlines, have motivated the organization of a dedicated “EBS-workshop” about cultural and natural heritage, which was held in January 2020 at the ESRF, attracting more than 150 participants, among which were 90 new ESRF users. Most of the talks were broadcast on the ESRF YouTube Channel and are still available (https://youtube.com/playlist?list=PLsWatK2_NAmyyA0n03OMJMAKobVivow2D). Through scientific presentations, tutorials, and discussions, the objectives of the workshop were:

1. To illustrate to expert and non-expert users the many capabilities offered by synchrotron radiation-based techniques for the study of natural and cultural heritage materials/objects;
2. To present EBS and the related instrumental developments, highlighting the ground-breaking capabilities that will be offered through the ESRF upgrade phase 2 (thanks to the new source, new beamlines, and new instruments);
3. To present and discuss the upstream and downstream challenges associated with these new instruments (e.g., access models and data analysis, data management...), which are fundamental for making the experiments a success. This was notably a very good opportunity to discuss the implementation of new beamtime access modes.

This event has been fundamental in some of the developments detailed in the following.

The new X-ray tomography beamline, BM18

CT provides the opportunity to visualize both external and internal structures non-invasively, which is particularly appealing for natural and cultural heritage. X-ray CT systems are now commonly found in natural history museums [2], and used in taxonomy [3], archeology [4], and paleontology [5]. The same trend is observed in institutes of cultural heritage [6], sometimes leading to the installation of bespoke setups adapted to special needs (e.g., [7, 8]). Characteristics of the X-ray beam generated by SR has attracted users in these communities, whether for the potential increase in resolution or solving problematic cases with higher energy and/or phase contrast imaging [1, 9].

Before the ESRF EBS upgrade, several beamlines were used for X-ray CT on natural and cultural heritage objects, namely BM05, ID17, and ID19 (not to mention ID16A and ID16B for nano-imaging). The three SR- μ CT beamlines had distinct characteristics (see table 1 in [1] for details). While each of these beamlines was very advantageous on its own, it was difficult to benefit from all of their properties simultaneously: ID19 offered high energy up to 250 keV and great spatial coherence but had a limited maximum beam size ($v \times h$: $12 \times 55 \text{ mm}^2$); BM05 and ID17 both proposed a much larger beam (up to $4 \times 100 \text{ mm}^2$ and $7 \times 150 \text{ mm}^2$ respectively) but were much more limited for using energies above 140 keV, and more importantly did not match the capabilities of ID19 for phase contrast imaging. The project of building BM18 aimed at increasing beam size with high energy and high coherence, together with increased available propagation distance to optimize propagation phase contrast imaging of large samples, taking full advantage of the exceptional coherence level offered on bending magnet ports with the new ESRF-EBS lattice.

One of the key developments on BM18 is the availability of a large beam size, which is currently measured at $18 \times 320 \text{ mm}^2$ ($v \times h$). The X-ray source is a tripole wiggler with the central pole at 1.56 T and two lateral poles at 0.85 T, which has been optimized for continuous hard X-ray spectrum. This wiggler provides the smallest possible source within the new ESRF EBS storage ring lattice, and the length of the beamline allows the sample to be placed at 172 m from the source. This insertion device is imperative to achieve the maximum level of coherence available on BM18 while expressing a large, high-energy beam (see [10] for more details). In the optics hutch, there are three sets of attenuators with five axes, each carrying filters composed of various materials (glassy carbon, Al, sapphire, fused silica, Cu, Mo, W) for beam attenuation and profiling, giving access to average energy up to 250 keV at lower resolutions and up to 150 keV at higher resolutions. The large beam size, together with the installation of a specialized large sample stage, which is planned for winter 2022, will give access to a vertical field of view of 250 cm for samples weighing up to 300 kg. Prior tomography experiments at the ESRF were restricted by the beam and sample stage sizes to a maximum sample diameter of 18 cm (e.g., [11, 12]), making impossible the imaging of many large and scientifically impactful natural and cultural heritage samples. The development and installation of a large beam size and large sample stage present ground-breaking and previously unattainable access to image such large and heavy objects.

Furthermore, samples can be imaged at multiple resolutions with an available voxel size from $120 \mu\text{m}$ to $0.6 \mu\text{m}$. These multiresolution capabilities will be made possible through a semi-automated detector stage with up to nine different detectors installed on it. The detector stage can move along the marble floor of the hutch on air pads, making it possible to cover propagation distances from 0 to 36 m. Two of the detectors allow for a continuous range of resolution selection from $25 \mu\text{m}$ to $1.4 \mu\text{m}$, enabling fast interchange between lower- and higher-resolution setups. This detector setup and adjustable propagation distance allows for a diversity in sample size imaging as well as the scan

of the same sample at many different resolutions. Hierarchical imaging allows for a precise location of small regions of interest for high-resolution imaging in much larger samples (Figure 1). The ability to gather data intensively on any given sample is important for the non-destructive study of rare and precious natural and cultural heritage samples.

Since its first application on fossils in 2003, phase contrast imaging rapidly appeared as a game-changer: in several paleontological cases, fossilized features that were invisible when using classical absorption-based X-ray CT appeared conspicuously when using propagation phase contrast SR- μ CT [9, 13]. BM18 was designed to ensure that phase contrast imaging would be usable with a much wider range of energies and resolution than before. The first prerequisite for this was to ensure sufficient spatial coherence of the beam, which depends on the X-ray source size and the distance between the source and the sample. Secondly, the sample-detector distance needed for propagation phase contrast increases the higher the energy but also the coarser the resolution: the experimental hutch is 45 m long, which allows us to move the large detector stage up to 36 m away from the sample.

In summary, BM18 provides unique opportunities for X-ray CT in natural and cultural heritage, allowing us to image larger and heavier samples at higher resolution and with a more efficient use of phase contrast imaging than anywhere in the world. Beyond the scientific advancement that the beamline provides, it also facilitates logistic issues: the range of resolution available allows collections of multiple datasets on a single sample without requiring any additional manipulation than the initial placement on the sample stage. It considerably expands the possibilities in these fields, especially with a beamline designed to accommodate a wide variety of samples, which is critical when dealing with samples that can rarely be altered for the sake of a single experiment.

New opportunities for micro- and nano-X-ray spectroscopic analyses

XAS-based techniques are now well-established for the chemical analysis of historical materials [14–16]. Determining the speciation of individual elements in a complex and heterogeneous matrix can reveal both the chemical fingerprint of the manufacturing processes (e.g., temperature and red/ox conditions during firing of glasses or ceramics) as well as characterization of degradation processes (e.g., reduction, oxidation, substitution reactions, modifying the chemical environment of the original materials). At the ESRF, the ID21 X-ray microscope is regularly used for application to cultural heritage, as it provides XAS capabilities in the tender X-ray range (2.1–10 keV) and sub-micrometric resolution [1, 17]. It is therefore possible to determine locally the speciation of elements (notably P, S, and the 3d transition metals), and to identify and map their various chemical forms over 2D cross-sections. A typical μ XRF/ μ XAS experiment is shown in Figure 2. From a first μ XRF map showing the distribution of elements of interest, points are selected on which μ XAS spectra are acquired (here points 1 and 2, Figure 2A). Degradation of historical materials are usually associated

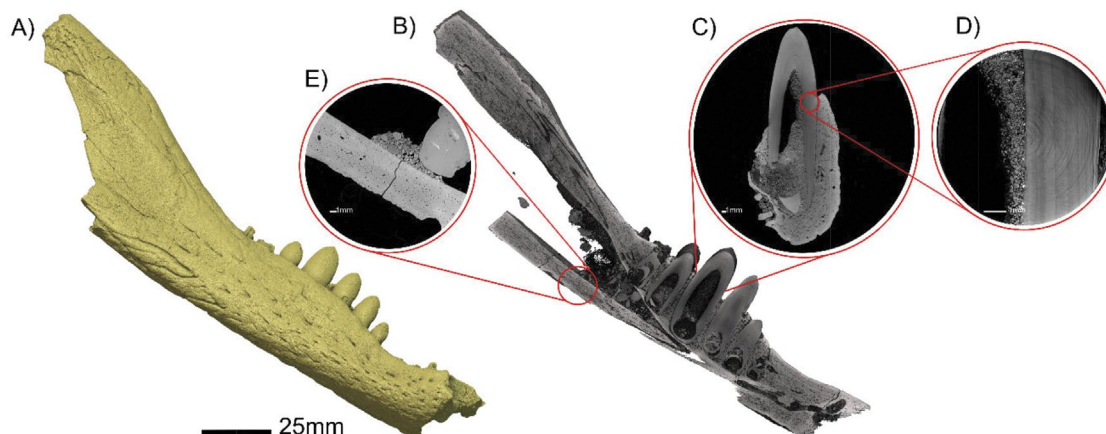


Figure 1: An illustration of the multiresolution capabilities of BM18 after the ESRF–EBS upgrade and the image quality resulting from increased X-ray coherence, optimized propagation distance, and energy. (A) The fossil scanned, reconstructed, and visualized is the jaw of *Antaeosuchus taouzensis* (22.72 μm , NHMUK-PV-R36874, Natural History Museum, London, UK), and is rendered in (B) lateral cross section, with (C) the largest tooth shown in cross-section apicobasally (22.72 μm). (D) In the tooth, a region of interest was located and scanned at 3.12 μm , and (E) in the jaw, a region of interest was located and scanned at 6.48 μm . Incremental lines in the tooth and growth lines in the jaw are already visible at 22.72 μm , which are both resolved further at their respective higher resolutions.

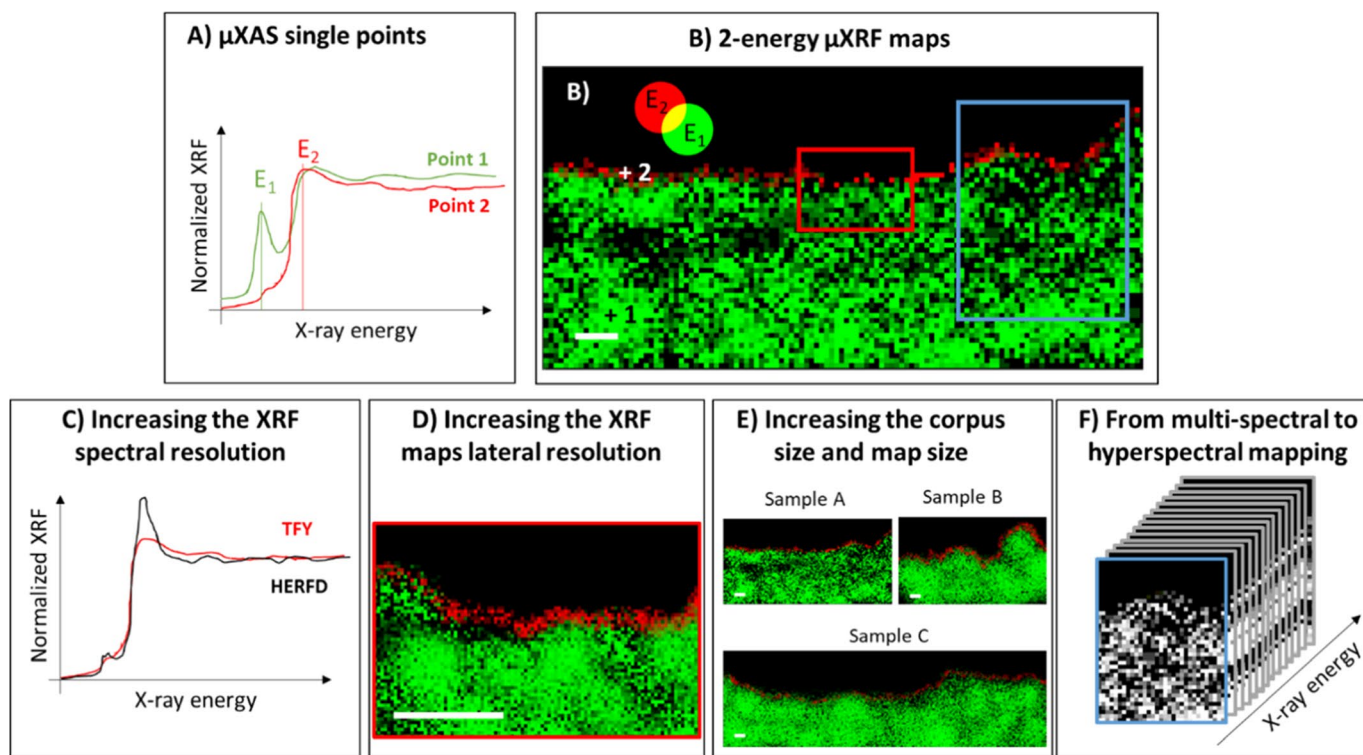


Figure 2: Sketch of a $\mu\text{XRF}/\mu\text{XAS}$ analysis of an historical sample (e.g., cross-section of a degraded painting) and the main benefits of the ESRF upgrade for such analyses. (A) Acquisition of individual μXANES spectra; (B) acquisition of 2-energy XRF maps; (C) comparison of XANES acquired with standard XRF energy dispersive detectors (total fluorescence yield) and with a crystal analyser (high-energy resolution fluorescence detection); (D) acquisition of XRF maps with increased lateral resolution (compared to B); (E) increasing the corpus and map size thanks to increased acquisition speed (compared to B); (F) acquisition of hyper-spectral XRF maps (same XRF map excited at tens energies). The different white bars scale to the same lateral dimension. See text for details.

with chemical alterations, highlighted by differences in XAS spectra. The original and degraded materials (here green and red, respectively) can be qualitatively mapped, under the assumption of a binary mixture, by acquiring the same μ XRF map at two energies, at least (here E_1 and E_2) (multi-spectral μ XRF mapping, Figure 2B). Thanks to the ESRF upgrade, such experiments can be revolutionized in several aspects. In particular, the ID21 beamline is now benefitting from an important refurbishment that is already profiting the heritage community. One of the first post-EBS experiments was conducted to understand the degradation of cadmium yellow paints in Picasso's paintings [18]. This was achieved by a combined S and Cl K-edges and Cd L_3 -edge μ XAS experiment, which strongly exploited the new performances of the beamline. Thanks to the new EBS source and its reduced horizontal emittance (decreased from 4 nm to 110 pm), notably from the reduced X-ray beam horizontal divergence, the X-ray beam was much more symmetric than previously (down to $0.36 \times 0.33 \mu\text{m}^2$ ($h \times v$)), which is extremely helpful for the study of highly heterogeneous paint samples. In addition, ID21 hosts the first prototype of the new generation of double crystal monochromators developed by the ESRF [19]. It delivers impressive beam stability, in both static and dynamic modes. For the experiment on Picasso's samples, the beam was kept stable within the beam size, while tuning the energy over the S K-, Cl K-, and Cd L_3 -edge ranges but also while switching from one edge to another (respectively 2.5, 2.9, 3.5 keV; i.e., Bragg angle 53, 43, 34° with Si(111) crystals). This is a real asset for multi-edges analyses, since it facilitates analyzing the speciation of various elements without losing time in beamline realignment and sample repositioning. Time was also saved thanks to the new graphical user interface (GUI), which offers an easy observation of the sample and selection of points and regions of interest, as well as easy tools for the selection of data acquisitions (single XAS scan, single 2D μ XRF maps and hyperspectral 2D μ XRF maps) [20]. This graphical interface, together with the new "Apache Guacamole" interface, allowed us to run the experiment mainly remotely during the lock-down period. The higher flux from EBS coupled to the new Falcon X readout electronics (Xia LLC) installed at ID21 have enabled us to collect XRF spectra with much shorter dwell times (down to ~ 10 ms). All of these developments make the beam smaller and more stable and the acquisitions faster, giving access to improved lateral resolution (Figure 2D) and increased sample corpus size and map size (Figure 2E). In addition, the increased speed will permit the use of hyperspectral mapping (acquisition of μ XRF maps excited at tens of energies, Figure 2F) in a more regular way, bridging the gap between high-resolution μ XRF 2D maps and high-quality single-point XAS. Finally, a new X-ray nanoscope is in development, which will complement and outperform the existing X-ray microscope, notably in terms of beam size and XRF collection. Thanks to all these developments, ID21 will keep and further increase its role within the heritage community.

In addition, the refurbished BM23 and ID24 XAS complex is also highly promising for the study of historical materials. It will complement ID21 very well thanks to access to higher energies (4 to 45 keV),

allowing us, for instance, to perform As K-, or Hg, Pb L-edges XAS analyses. In addition, the possibility to combine the small X-ray focal spot ($500 \times 500 \text{nm}^2$ FWHM) with the high-energy resolution fluorescence detection (HERFD) offered by the crystal analyzers is a strong asset, in particular for the characterization of diluted, complex, and heterogeneous materials, where the same element can be present under several speciations. Subtle XAS differences that could be difficult to detect with standard total fluorescence yield (TFY) can be better highlighted thanks to HERFD (Figure 2C). These two beamlines are also equipped with 2D detectors, allowing combined XRD capabilities.

New opportunities for micro-X-ray diffraction analyses

XRPD-based techniques are also very well-suited for the determination of the composition of historical materials, in particular the crystalline components. At the ESRF, two complementary XRPD-based techniques are increasingly used by the cultural heritage community: high angular resolution X-ray powder diffraction (HR-XRPD) and micro X-ray powder diffraction (μ XRPD) mapping. The former offers accurate characterization of crystalline materials (e.g., identification and quantification, structure refinement and crystallite size determination, description of the crystallographic structure). The latter provides more qualitative information but with additional insight into the 2D or 3D distribution of crystalline phases at the micrometer scale. As an example, these two techniques were recently successfully combined to reveal different lead white qualities in old Masters paintings [21] as well as to identify a very unusual lead compound, plumbonacrite, in Rembrandt's impastos [22].

The application of μ XRPD mapping to historical paintings was pioneered about 15 years ago, but at that time the relatively low speed (~ 10 s/pixel) restricted its performances [23]. Nowadays, thanks to the increase of flux offered by EBS, the availability of fast pixel-array detectors in combination with fly-scan capability, similar experiments can be performed at a speed down to ~ 10 ms/pixel. However, the time spent in writing a two-page proposal, completing its technical and scientific review, planning the experiment, setting up the beamline, etc., stays fundamentally the same. Taking into account the increasing interest of the heritage community in these techniques and the decreasing acquisition time, it was therefore necessary to reconsider the beamtime access mode for this type of experiment. Inspired by the success of the block allocation group (BAG) system to schedule beamtime used in structural biology for several years, the implementation of an "historical materials BAG" was discussed at the "Heritage EBS Workshop" (see earlier in this article). A "pre-BAG" proposal was successfully submitted in 2020 followed by the final BAG project in 2021 [24]. This is one of the three new access modes pioneered at the ESRF in 2020 [25]. Within the BAG, different scientific projects are grouped together that all require structural information obtainable by XRPD at the ESRF, either through μ XRPD/ μ XRF mapping at ID13 (beam $\sim 2 \times 2 \mu\text{m}^2$) or HR-XRPD at ID22 (instrumental function 2θ full width at half maximum

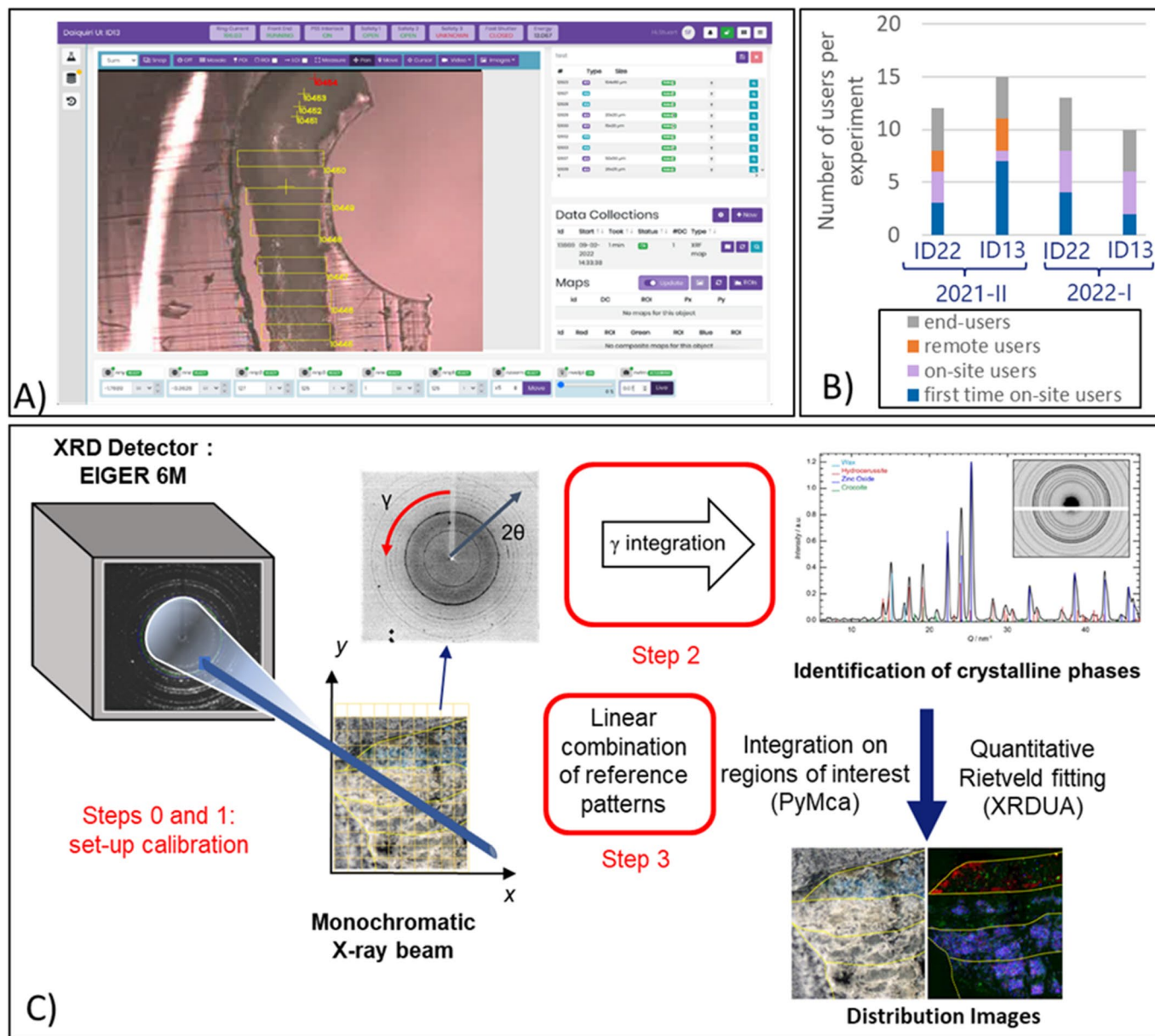


Figure 3: Three important software developments facilitating data acquisition and processing. (A) The ID13 graphical user interface, Daiquiri; (B) the remote access; (C) the Jupyter Notebooks for setup calibration, azimuthal integration, and fit by linear combination.

of (111) Si peak, $\sim 0.0027^\circ$). Regular access is provided to ID13 (12 shifts) and ID22 (6 shifts) every six months and for a 2-year period (2021–2023). The BAG is renewable upon request and reviewed at the end of the 2-year period. The initial BAG was co-submitted by 11 European institutes (Rijksmuseum, Amsterdam, The Netherlands; TU Delft, The Netherlands; CNR-SCITEC, Perugia; Courtauld Institute of Art, London, UK; Politecnico di Milano; Centre de Recherche et de Restauration des Musées de France, Paris, France; Institut de Recherche de

Chimie de Paris, Paris, France; Universitat Politècnica de Catalunya, Barcelona, Spain; University of Antwerp, Belgium, the CNRS, Paris and the ESRF, Grenoble, France), but many more institutes have benefited from the BAG access via collaborations with the main partners.

The success of the BAG fundamentally relies on the efficiency of data acquisition. High throughput can be reached thanks to the efficiency of the X-ray instruments themselves, but also by optimizing sample mounting and data collection. At ID22, this is notably ensured

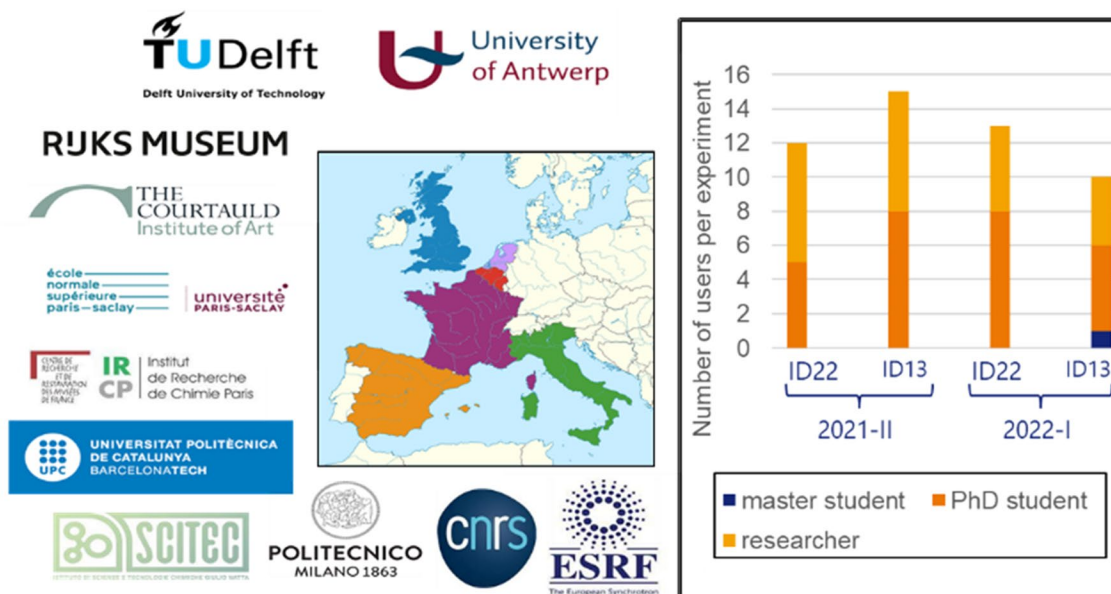


Figure 4: The different partners of the Historical Materials BAG and some statistics about users over the first four beamtimes.

via a robot, which can handle up to 75 capillary samples. At ID13, specific sample holders were designed for the BAG project, allowing the mounting of up to 54 tiny ($< 3 \times 3 \text{ mm}^2$) samples (cross-sections or thin sections mainly) together. The BAG also motivated the deployment of the Daiquiri graphical user interface at ID13. It allows observing and navigating samples, selecting points of interest and regions of interest, defining and launching long series of scans [20] (Figure 3A). The interface is very intuitive and new users can be autonomous within few minutes. μ XRD intensity maps can be displayed in real time, superimposed on the optical image of the samples. In addition, in response to lockdowns, the ESRF has implemented remote access (Figure 3B). Users can join the experiment from their lab or their home and use the graphical interface similarly. These two aspects have been crucial in pushing the accessibility of the beamlines to BAG partners.

Downstream data acquisition, efforts have been dedicated to optimize and stabilize data processing and analysis, notably via Jupyter notebooks for data processing of ID13 XRD patterns, based on the PyFAI software package [26] (Figure 3C). Basically, different notebooks have been written for: (0) and (1) the calibration of the setup; (2) the azimuthal integration of XRPD patterns; (3) the fit of patterns as linear combinations of a set of references. Additional features are in development. The processing notebooks are open-source and freely available at <https://gitlab.esrf.fr/loic.huder/juno> [24].

After only 1 year (two beamtime experiments at the two beamlines), 29 users have already benefitted from this facilitated access. This represents seven countries, with a total of 336 samples at ID13 and 161 samples at ID22 that have been analyzed. Interestingly, beyond the global gain of efficiency of the entire beamtime process (proposal submission,

evaluation, scheduling, beamline setup...), this collective access has demonstrated a real opportunity to train new users, in particular young scientists, on the various aspects of synchrotron experiments: sample preparation, data acquisition, data processing, data analysis. As shown in Figure 4, more than half of the on-site users were first-time users, and more than half of the users are Ph.D. students or master students. In addition to the organization of tutorials and hands-on practicals at the beamline, the BAG has revealed a real strength in developing a European network among these (young) researchers, who naturally collaborate from the preparation of the experiments to the analysis of the results.

Different examples of applications can be found in the reference publication [24], notably the study of (1) the manufacturing processes and composition of cadmium red pigments; (2) the origin of the color of “Thénard’s Blue,” from the Manufacture Nationale de Sèvres; (3) the structural damage in wood vessels; (4) the interactions of inorganic conservation treatments with Mg-containing frescos; and (5) the degradation of cadmium yellow in Picasso’s paintings. The last two works are further detailed in recent publications [18, 27].

Conclusions

As is clear from this article, the cultural and natural heritage community is extensively using the ESRF. Thanks to the EBS source, the implementation of state-of-the-art beamlines, such as BM18, the continuous refurbishment of existing beamlines, and the development of adapted access models, ESRF offers a very appealing context for this community. Beyond instrumentation and methodology development,

the cooperative spirit that has been developed between the facility and its users is fundamental. Outreach and training activities have been key in strengthening the link with users and attracting new collaborations. BAG turns out to be a fantastic example of a partnership between the ESRF and a user community, defining and developing together new working models. Undoubtedly, this cooperation shall further contribute directly and indirectly in raising cultural knowledge.

Acknowledgments

The authors thank users and colleagues for their involvement and contributions in all of the activities described in this article. In particular, CD thanks A. Fitch for his support at ID22 and PT warmly thanks J. Baruchel for his constant support in the development of the paleontology at the ESRF.

Funding

The Historical Materials BAG is supported by the Streamline project, Horizon 2020 funded project (INFRADEV grant agreement No 870313). LH is funded via the PANOSC project (European Union's Horizon 2020 Research and Innovation program under Grant Agreement No. 823852). IF is funded via the European Union's Horizon 2020 research and innovation program under the Marie Skłodowska-Curie grant agreement No 847439. VG is funded by the European Union's Horizon 2020 research and innovation programme under the Marie Skłodowska-Curie actions (Grant Agreement #945298-ParisRegionFP). ■

References

- M. Cotte et al., *Synch. Radiat. News*. **32** (6), 34 (2019). doi:10.1080/08940886.2019.1680213
- K. Keklikoglou et al., *Eur. J. Taxonom.* **522**, 1–55 (2019). doi:10.5852/ejt.2019.522
- S. Faulwetter et al., *ZK*. **263** (263), 1 (2013). doi:10.3897/zookeys.263.4261
- R. L. Abel et al., *Comput. Graphic.* **35** (4), 878 (2011). doi:10.1016/j.cag.2011.03.001
- M. Sutton et al., *Paleontol. Soc. Pap.* **22**, 1 (2016). doi:10.1017/scs.2017.5
- A. M. C. A. N. 98, *Anal. Method.* **12** (36), 4496 (2020).
- F. Albertin et al., *Heritage*. **2** (3), 2028 (2019). doi:10.3390/heritage2030122
- A. Masson-Berghoff et al., *Br Mus Stud Ancient Egypt Sudan*. **24**, 159 (2019).
- P. Tafforeau et al., *Appl. Phys. A*. **83** (2), 195 (2006). doi:10.1007/s00339-006-3507-2
- F. Cianciosi et al., eds., BM18, the new ESRF-EBS beamline for hierarchical phase-contrast tomography In *11th Mechanical Engineering Design of Synchrotron Radiation Equipment and Instrumentation (MEDSI'20)*, Chicago, IL, USA, 24–29 July 2021. (JACOW Publishing, Geneva, Switzerland, 2021).
- K. J. Carlson et al., *Science*. **333** (6048), 1402 (2011). doi:10.1126/science.1203922
- V. Fernandez et al., *PLoS One*. **8** (6), e64978 (2013). doi:10.1371/journal.pone.0064978
- V. Fernandez et al., *Microsc. Microanal.* **18** (1), 179 (2012). doi:10.1017/S1431927611012426
- M. Cotte et al., *Acc. Chem. Res.* **43** (6), 705 (2010). doi:10.1021/ar900199m
- K. Janssens et al., Using synchrotron radiation for characterization of cultural heritage materials, in: E. Jaeschke et al., eds., *Synchrotron Light Sources and Free-Electron Lasers: Accelerator Physics, Instrumentation and Science Applications*. (Cham: Springer International Publishing 2019), pp. 1–27.
- F. Farges et al., X-ray absorption spectroscopy and cultural heritage: Highlights and perspectives, in *X-Ray Absorption and X-Ray Emission Spectroscopy: Theory and Applications* (Chichester (UK): John Wiley & Sons, 2016), pp. 609–636.
- M. Cotte et al., *J. Anal. At. Spectrom.* **32** (3), 477 (2017). doi:10.1039/C6JA00356G
- M. Ghirardello et al., *Microsc. Microanal.*, **28** (5), 1504–1513 (2022). doi:10.1017/S1431927622000873
- R. Baker et al., eds., ESRF double crystal monochromator prototype project *Mechanical Eng. Design of Synchrotron Radiation Equipment and Instrumentation (MEDSI'18)*, Paris, France, 25–29 June 2018. (Geneva, Switzerland: JACOW Publishing, 2018).
- S. Fisher et al., *J. Synchrotron Rad.* **28** (6), 1996 (2021). doi:10.1107/S1600577521009851
- V. Gonzalez et al., *Anal. Chem.* **89** (5), 2909 (2017). doi:10.1021/acs.analchem.6b04195
- V. Gonzalez et al., *Angew. Chem. Int. Ed.* **58** (17), 5619 (2019). doi:10.1002/anie.201813105
- M. Cotte et al., *J. Anal. At. Spectrom.* **23** (6), 820 (2008). doi:10.1039/b801358f
- M. Cotte et al., *Molecules* **27** (6), 1997 (2022). doi:10.3390/molecules27061997
- J. McCarthy et al., *Synchrot. Radiat. News*. **35** (2), 52 (2022). doi:10.1080/08940886.2022.2064150
- J. Kieffer et al., *J. Synchrotron Rad.* **27** (2), 558 (2020). doi:10.1107/S1600577520000776
- N. Oriols et al., *Cem. Concr. Res.* **157**, 106828 (2022). doi:10.1016/j.cemconres.2022.106828